

# Water removal characteristics of proton exchange membrane fuel cells using a dry gas purging method

Sang-Yeop Lee<sup>a</sup>, Sang-Uk Kim<sup>a,b</sup>, Hyoung-Juhn Kim<sup>a</sup>, Jong Hyun Jang<sup>a</sup>,  
In-Hwan Oh<sup>a</sup>, Eun Ae Cho<sup>a</sup>, Seong-Ahn Hong<sup>a</sup>, Jaejun Ko<sup>c</sup>,  
Tae-Won Lim<sup>c</sup>, Kwan-Young Lee<sup>b</sup>, Tae-Hoon Lim<sup>a,\*</sup>

<sup>a</sup> Center for Fuel Cell Research, Korea Institute of Science and Technology, 39-1 Hawolgok-dong, Sungbuk-gu, Seoul 136-791, South Korea

<sup>b</sup> Department of Chemical Engineering, Korea University, Anam-dong, Sungbuk-gu, Seoul 136-701, South Korea

<sup>c</sup> Fuel Cell Vehicle Team 1, Hyundai-Kia Corporate Research and Development Division, 104 Mabuk-Dong, Giheung-Gu, Yongin-Si, Gyeonggi-do 446-912, South Korea

Received 1 November 2007; received in revised form 2 January 2008; accepted 4 January 2008

Available online 12 January 2008

## Abstract

Water removal from proton exchange membrane fuel cells (PEMFC) is of great importance to improve start-up ability and mitigate cell degradation when the fuel cell operates at subfreezing temperatures. In this study, we report water removal characteristics under various shut down conditions including a dry gas-purging step. In order to estimate the dehydration level of the electrolyte membrane, the high frequency resistance of the fuel cell stack was observed. Also, a novel method for measuring the amount of residual water in the fuel cell was developed to determine the amount of water removal. The method used the phase change of liquid water and was successfully applied to examine the water removal characteristics. Based on these works, the effects of several parameters such as purging time, flow rate of purging gas, operation current, and stack temperature on the amount of residual water were investigated.

© 2008 Elsevier B.V. All rights reserved.

**Keywords:** Cold start-up; Dry gas purging; Freeze-thaw cycles; Proton exchange membrane fuel cell (PEMFC)

## 1. Introduction

There are several technical barriers to be overcome before commercializing proton exchange membrane fuel cells (PEMFC) as power sources in automobiles, even though they have advantages such as cleanliness and high efficiency. One of the emerging problems is their operation in cold climates. PEMFCs are mainly operated in the temperature range of 60–80 °C, but it is common for them to shut down and start-up fuel cells under subfreezing temperatures. Several studies revealed that the residual water in the fuel cell hinders cold start-up and causes irreversible degradation of PEMFCs when they are kept in subfreezing temperatures [1–8].

The main cause of cell degradation, which occurs under subfreezing temperatures, is ice formation. It physically damages the cell components, such as gas diffusion media (GDM), the catalyst layer, and the electrolyte membrane. First, when volume expansion due to the ice formation occurs in the GDM, the hydrophobic material coated on carbon fibers is delaminated and the pore structure is destructed. Oszcipok et al. showed by using contact angle measurements that the hydrophobicity of the GDM was appreciably reduced along flow patterns after operation at temperatures below 0 °C [5]. They reported that water droplets agglomerated along flow patterns in the GDM of the cathode side, which indicates that the hydrophobic treatment was degraded. In addition to the contact angle measurements, SEM evaluations confirming damage of the GDM were performed by Yan et al. [6]. Second, the interface between a membrane and catalyst layers is also deteriorated by ice lens formation. Several studies have shown that a catalyst layer was delaminated

\* Corresponding author. Tel.: +82 2 9585273; fax: +82 2 9585199.  
E-mail address: [thlim@kist.re.kr](mailto:thlim@kist.re.kr) (T.-H. Lim).

from the membrane because of the frost heave mechanism due to ice lens formation [1,6–9]. Cho et al. carried out two different kinds of freeze-thaw cycles: one contained a water-removal step in the shut down procedure and the other did not. When water was not removed from fuel cell, the ohmic and charge transfer resistance increased significantly after four freeze-thaw cycles whereas no performance degradation was observed when the water removal step was adopted [3]. Third, ice formation also degrades the membrane. Yan et al. observed pin holes in the membrane near cathode outlet regions after operation at  $-15^{\circ}\text{C}$  [6]. Considering these several studies, there seem little doubt that water removal is essential in order to mitigate the physical deterioration of fuel cell components.

Water removal in the shut down process is essential not only to prevent cell degradation but also to improve the start-up ability under cold conditions. Oszcipok et al. examined the relation between the start-up ability and operating conditions using statistical methods [5]. They concluded that a drier membrane is extremely advantageous to start-up PEMFCs at subfreezing temperatures since heat generation originating from ohmic losses is large when the membrane is dry. Moreover, in the same article, the authors observed, with pressure drop measurements, that gas channels were blocked with ice, resulting in start-up failure and electrode deterioration due to localized fuel starvation. The water removal at shut down could reduce the channel blockage in a cold start-up. In addition, if there is a significant amount of water in the fuel cell stack, the water acts as a thermal mass, resulting in an obstacle for cold start-up.

Purging dry gas in the shut down step is one of the simplest and most effective ways to remove water from the fuel cell stack [3,10–12]. It was reported that the purging method is able to prevent cell degradation due to ice formation [3]. In addition, the purging method has a distinct advantage in that the power systems do not need to adopt extra devices. Even though it is most beneficial to completely remove water, this requires much energy and time. In order to reduce parasitic energy losses and enhance the user's convenience, a purging method that consumes less energy and requires less time should be developed. Therefore, the characteristics of water removal by dry gas purging must be investigated. In this report, the ohmic resistance and the total amount of residual water were measured to investigate the effects of purging time, the flow rate of purging gas, the operation current, and the stack temperature on the water removal.

## 2. Experimental

### 2.1. Stack fabrication and operating conditions

A PEMFC short stack consisting of three cells was fabricated. The cells consisted of commercially available MEA ( $250\text{ cm}^2$ ), gas diffusion media (GDM), and bipolar plates. The assembled stack was activated for 24 h with fully humidified hydrogen and air.

Prior to the shut down process, the PEMFC stack was operated at  $65^{\circ}\text{C}$  for 90 min to generate and distribute water in the stack. The reactant gases were fully humidified in a bubbler type humidifier whose temperature was  $65^{\circ}\text{C}$ . After the oper-

ation, we executed the shut down process, which consisted of disconnecting the load and purging dry nitrogen with these two operations being carried out simultaneously. The electronic load was decreased to zero, and dry nitrogen was supplied to the stack to discharge water.

### 2.2. Measurement of residual water

The dehydration level of the electrolyte membrane and the total amount of residual water were measured to examine the water removal characteristics. First, a milliohm meter (Hioki 3560) was employed to observe the resistance of the membrane. The measured resistance can be converted to the hydration level of the membrane by applying an empirical correlation between proton conductivity and water content [13].

In order to measure the total amount of residual water in the stack, a novel method using the phase change of liquid water to gas was developed. The main idea of the method is that the amount of water can be estimated by considering the change of internal pressure in the stack after all of the water in the stack evaporates. However, it is difficult to completely vaporize liquid water under moderate temperatures. As liquid water is changed to vapor, the pressure in the stack rises exceedingly so that the boiling point of water rises above  $100^{\circ}\text{C}$ . Therefore, the temperature of the stack should be maintained much higher than  $100^{\circ}\text{C}$  to vaporize all of the liquid water even though keeping the cell above  $200^{\circ}\text{C}$  causes deterioration of sulfonic acid groups in the polymer electrolyte.

To solve this problem, it was considered that the boiling point decreases consistently with pressure. Fig. 1 represents the principles of the method. Two vacuum tanks with internal volumes of 40 L each were employed to depressurize the stack: one was used for the anode, and the other was used for the cathode. The tanks were purged with dry nitrogen with a flow rate of  $10\text{ L min}^{-1}$  for an hour in a climate chamber at  $100^{\circ}\text{C}$  to completely eliminate water. Then, the nitrogen was evacuated from the tanks

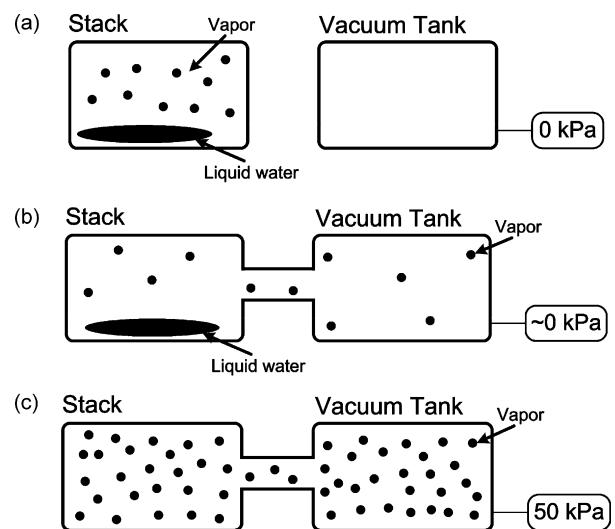


Fig. 1. Principles of the method using the phase change of water for the measurement of residual water: (a) before connecting the stack to vacuum tanks, (b) immediately after connecting, and (c) equilibrium state.

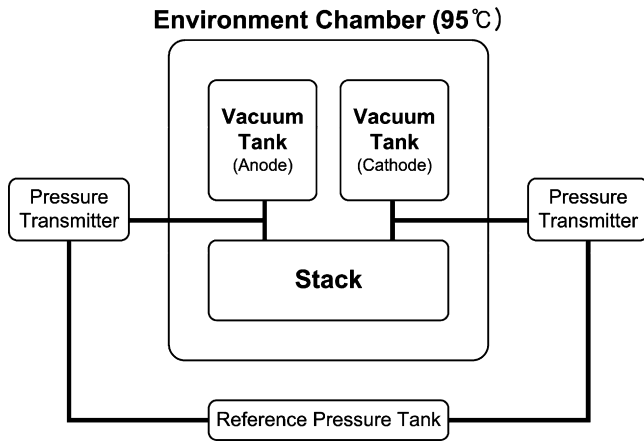


Fig. 2. Schematic sketch of experimental devices for measuring the amount of residual water.

by a diaphragm pump. After the fuel cell stack was operated under specific conditions, it was transferred and connected to the two tanks, which were kept under reduced pressure in the climate chamber (Fig. 1(b)). The stack and tanks were maintained at 95 °C for a few hours in the climate chamber to attain an equilibrium state (Fig. 1(c)). Fig. 2 shows the entire set of devices used for the measurement. The climate chamber was used to constantly maintain the temperature of the stack and tanks. Pressure difference transmitters and a reference pressure tank were applied to observe the internal pressure change in the stack.

### 3. Results and discussion

#### 3.1. Estimation of water content in the electrolyte membrane by measuring the resistance of the stack

The proton conductivity of perfluorosulfonated polymers such as Nafion depends on the amount of water in the polymer. Springer et al. provided an empirical correlation between the number of water molecules in each sulfonic acid group ( $\lambda$ ) and proton conductivity ( $k$ ) [13]. They reported that proton conductivity has a linear dependency on  $\lambda$

$$k = (0.5139\lambda - 0.326) \exp \left[ 1268 \left( \frac{1}{303} - \frac{1}{T} \right) \right] \left[ \frac{S}{m} \right] \quad (1)$$

where  $T$  is the temperature. Using this relationship, the membrane dehydration level can be estimated by measuring the resistance.

However, the measured resistance is attributed not only to the electrolyte as discussed previously but also to the contact resistance. Thus,

$$\begin{aligned} \text{Measured resistance} &= \text{membrane resistance} \\ &+ \text{contact resistance} \end{aligned} \quad (2)$$

Therefore, to accurately calculate the membrane dehydration level, it is required to subtract the contact resistance from the measured resistance. The contact resistance occurs at interfaces between a bipolar plate and GDM as well as between GDM

and the catalyst layer. Measurement of the contact resistance between a bipolar plate and GDM is comparatively easy and has already been performed in many studies [14–16]. On the contrary, it is not simple to directly measure the contact resistance between GDM and a catalyst layer.

We measured the high frequency resistance (HFR) of the fuel cell stack under different humidity conditions to estimate the contact resistance and validate Eq. (1). Humidified nitrogen was fed to the fuel cell stack with flow rates of 5 L min<sup>-1</sup> for the anode and cathode, while the temperature of the stack was maintained at 65 °C. The relative humidity of the nitrogen gas was varied using values of 63, 70, 80, 88, and 100% at 65 °C. Under the condition that membrane reaches equilibrium with humid nitrogen, these humidity conditions can be converted to  $\lambda$  values by the correlations below [13]:

$$\begin{aligned} \text{if } 0 < a \leq 1, & \quad \lambda = 0.043 + 17.18a - 39.85a^2 + 36.0a^3 \\ \text{if } 1 \leq a \leq 3, & \quad \lambda = 14 + 1.4(a - 1) \end{aligned} \quad (3)$$

where  $a$  is the water activity, which is defined as water vapor pressure divided by the saturated water vapor pressure. By using Eq. (3), the relative humidities of 63, 70, 80, 88, and 100% result in  $\lambda$  values for the electrolyte membrane of 4.05, 4.87, 6.64, 8.83, and 13.37, respectively.

A plot of  $\lambda$  versus measured resistance (■) is presented in Fig. 3. The resistance values calculated by Eq. (1) (○) and the differences between the total and the electrolyte membrane resistances (△) are also shown in Fig. 3. Firstly, the calculated membrane resistances show a similar tendency to the measured ones. In addition, the differences between the measured stack resistances and the predicted electrolyte membrane resistances varied only slightly by changing the gas humidity. The average value was 0.7140 mΩ with a standard deviation of only 0.030 mΩ. Therefore, it can be concluded that Eq. (1) agrees well with the experimental results and the contact resistance of the stack is estimated as 0.7140 mΩ.

Based on the measured contact resistance and Eq. (1), an empirical correlation between the water content in the membrane

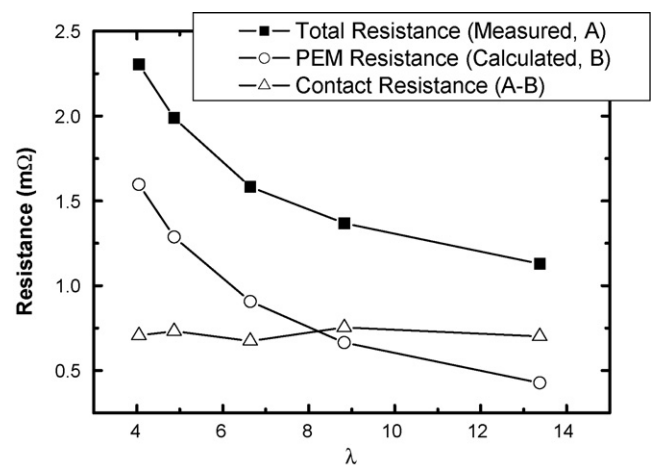


Fig. 3. Comparison of the measured stack resistance, the electrolyte membrane resistance predicted by Eq. (1), and the estimated contact resistance as a function of  $\lambda$ .

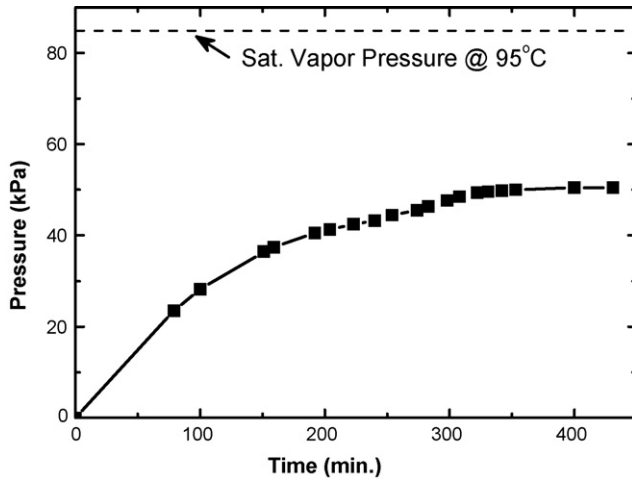


Fig. 4. Pressure built by vaporization after the stack was connected to the vacuum tanks.

( $\lambda$ ) and the stack resistance ( $r$ ) was derived as follows:

$$r(\text{m}\Omega) = 0.7140 + \frac{4.32}{0.7926\lambda - 0.5028} \quad (4)$$

### 3.2. Measurement of the amount of residual water

The stack was operated at a constant current load of 175 A for 90 min and purged for a minute with dry nitrogen at flow rates of 3.1 and 9.9 L min<sup>-1</sup> for the anode and cathode, respectively. Then, the stack was transferred and connected to two vacuum tanks, which were described in Section 2, in the climate chamber at 95 °C. Fig. 4 displays the internal pressure change of the stack after it was connected to the tanks in the climate chamber. The internal pressure was almost zero immediately after the connection because the overall internal volume of the vacuum tanks was much bigger than that of the stack. The overall volume of the vacuum tanks was 80 L while that of the stack was only 141 mL. After 400 min, the pressure did not increase further, which means the system reached equilibrium. The fully developed pressure was 50.4 kPa, which is smaller than 84.55 kPa, which is the saturated vapor pressure at the temperature in the climate chamber (95 °C) [17]. Therefore, we can conclude that all of the liquid water in the stack evaporated into vapor.

Using the ideal gas equation, the amount of residual water can be calculated from the changes in vapor pressure. To examine the accuracy of the ideal gas equation, comparisons between values calculated by the equation and those obtained from experiment were carried out. The results are presented in Table 1. From the table, the differences between the calculated and experimental

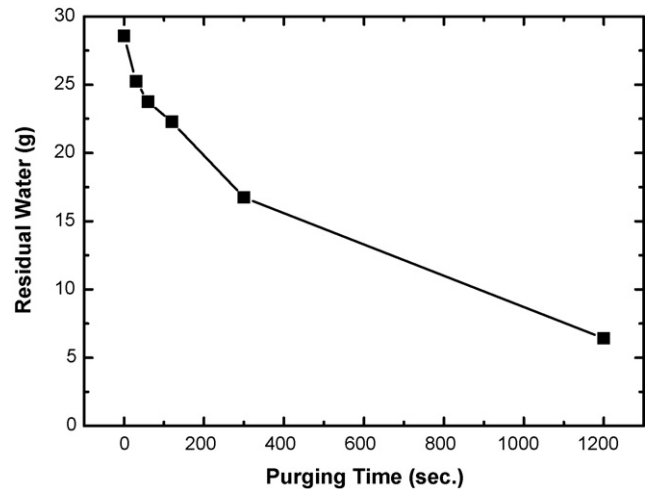


Fig. 5. Water removal by dry nitrogen purging with different execution times.

values are so small that the ideal gas equation is suitable for calculating the amount of water from the vapor pressure.

### 3.3. Effect of purging time

Water removal was examined using different purging times in order to investigate the effect of purging time on the amount of residual water. As described in Section 2, prior to shut down, the stack was operated at 65 °C with fully humidified hydrogen and air (operation current: 175 A). After the operations, dry nitrogen was purged for the following durations: no purge, 30, 60, 120, 300, and 1200 s. The flow rates of nitrogen were 3.3 and 9.9 L min<sup>-1</sup> for the anode and cathode, respectively.

Fig. 5 shows the total amount of residual water after applying the different nitrogen purging times. When the purge process was not executed at all, the amount of residual water was 28.58 g. Since the internal volume of the stack was 141 mL, about 20% of the total volume was filled with liquid water during the operation. While water was rapidly discharged from the stack in 60 s, the water removal rate decreased gradually as the nitrogen purging was extended further. Even though the stack was purged with dry gas for 1200 s, 6.42 g of water remained in the stack.

The dehydration characteristic of the electrolyte membrane as a function of purging is given in Fig. 6. Using Eq. (4),  $\lambda$  is presented on the right axis of the graph (a). As purging time increased, the resistance increased. The  $\lambda$  of the electrolyte membrane reached 4 in 100 s. After 120 s, the resistance surged upwards drastically because proton conductivity became very low. It was determined that the membrane was almost dehydrated in 300 s. However, according to Fig. 5, a significant

Table 1

Comparison between values calculated by the ideal gas equation and those obtained by experiment

Temperature (°C)	40	60	80	100
Saturated vapor pressure (kPa) [17]	7.384	19.940	47.39	101.350
Specific volume of vapor from the property table (m <sup>3</sup> kg <sup>-1</sup> ) [17]	19.52	7.671	3.407	1.6729
Specific volume of vapor from the ideal gas equation (m <sup>3</sup> kg <sup>-1</sup> )	19.579	7.714	3.441	1.7000
Error (%)	0.30	0.56	0.98	1.24

amount of liquid water still existed in the fuel cell stack after purging for 300 s. This means that liquid water in GDM, channels, or manifolds was barely removed while the membrane was dehydrated.

Although the electrolyte membrane seemed to be dehydrated while purging was executed, the resistance decreased immediately after purging was stopped (Fig. 6). The rapid decrease of resistance may be attributed to the remaining water as shown in Fig. 5. After purging was stopped, the residual water may be well dispersed so that the membrane was hydrated again.

### 3.4. Effect of flow rate of purge gas and purging time

We investigated which is the more influential parameter on water removal between the flow rate of the purge gas and the purging time. To study the effects of these parameters, four different purging methods were carried out. We fixed the total amount of purging gases by changing the flow rate of the purge gas and the purging time. As the flow rate increased, the purging time was shortened to keep the total amount of purging gas constant. The purging cases are presented in Fig. 7. The 1Q represents flow rates of 1.6 and 5.0 L min<sup>-1</sup> for the anode and cathode, respectively. As mentioned in the previous section,

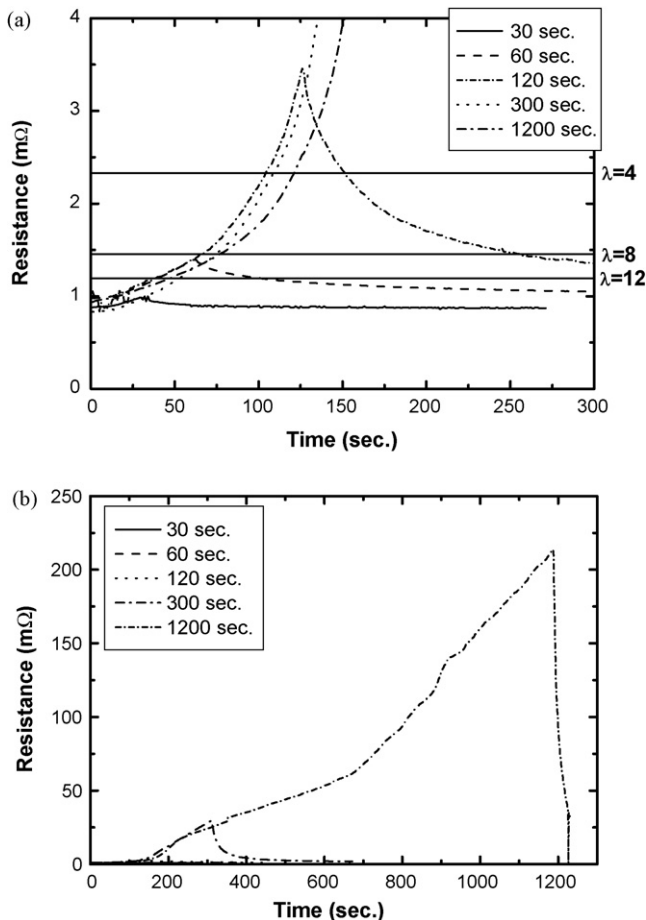


Fig. 6. The electrolyte membrane dehydration by dry nitrogen purging: (a) magnified and (b) original figures.

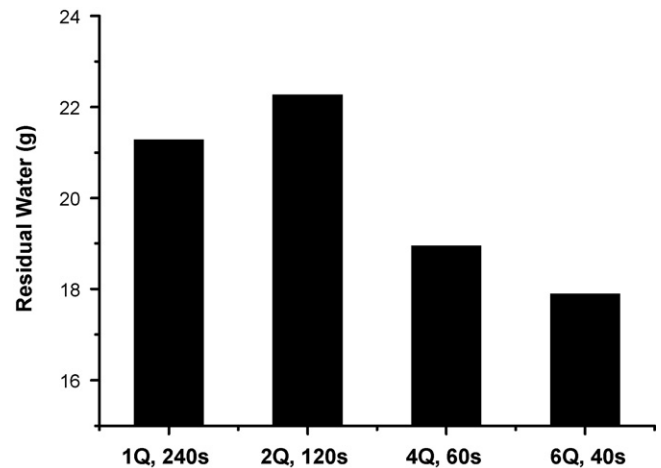


Fig. 7. Effect of the purge gas flow rate and purge time on the amount of residual water.

purging was carried out after the stack had been operated at 175 A for 90 min. The residual water amounts for the four cases are presented in Fig. 7. It was found that increasing the flow rate is extremely advantageous compared to extending the purging time to remove the water in the stack if the same amount of purging gas was used. The reason why water removal is more efficient at higher flow rates might be the gas speed in the gas channels of the stack. There are two mechanisms by which the dry nitrogen stream removes water from the fuel cell stack: vaporization and physically pushing liquid water droplets. In the case of the latter, stagnation pressure built up by the gas stream should be larger than the retention force between water droplets and the channel walls to remove the droplets in the gas channels. Since the stagnation pressure is directly proportional to the square of gas velocity, the flow rate is a primary factor affecting water removal.

Fig. 8 shows changes in ohmic resistance. The increasing rate of resistance was significantly larger with high flow rates than with low flow rates. However, as shown in Fig. 6, the electrolyte membrane was hydrated again after purging was completed.

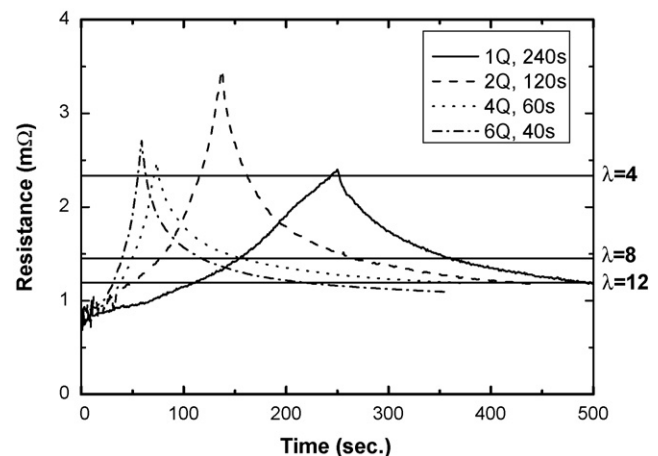


Fig. 8. Effect of purge gas flow rate and purge time on the electrolyte membrane dehydration.

### 3.5. Effect of operation current

The amount of residual water may be affected by the operation current since the water production rate is directly proportional to current. To investigate the effects of the operation current on the amount of residual water, the stack was operated at 30, 100, 175, 240, and 300 A. Fully humidified hydrogen and air with stoichiometries of 1.5 and 2.0 for the anode and cathode, respectively, were used for the operation. After operation, dry nitrogen was supplied for 5 min with flow rates of 3.3 and 9.9 L min<sup>-1</sup> for the anode and cathode, respectively.

Fig. 9 shows the amount of residual water in the purged and non-purged fuel cell stacks. First, when the purging was not executed, it is observed that the amount of residual water decreased with an increasing operation current. This might seem to be contradictory since the rate of water generation is directly proportional to current. However, it should be noticed that hydrogen and air flow rates are also directly proportional to current because the stoichiometries were fixed at 1.5 and 2.0 for the anode and cathode, respectively. The ratio of the amount of gas supplied to water generation was constant regardless of current. The high flow rate in the case of high current operation might be advantageous in water removal during stack operation. As mentioned in Section 3.4, gas streams with high speeds in the channels might be able to effectively push liquid water droplets to the outlet. Also, the amounts of residual water after purging decreased as the operation current increased. It was observed that 40.5% of the initial residual water was removed after the purging with operation at 30 A.

Fig. 10 presents the effects of varying the operation current on membrane dehydration. The electrolyte membrane dehydration occurred rapidly when the operation current was high. This phenomenon is considered to be caused by differences of residual water right before the purging step. However, the membrane hydration occurred again just after purging was finished. In conclusion, in the case of low current operation such as the parking mode of automobiles, the amount of residual water is so large that a rigorous water removal process should be adopted.

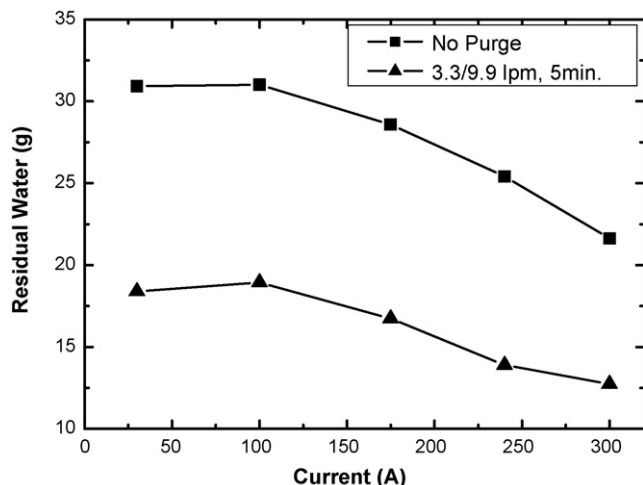


Fig. 9. Effect of operation current on the amount of residual water.

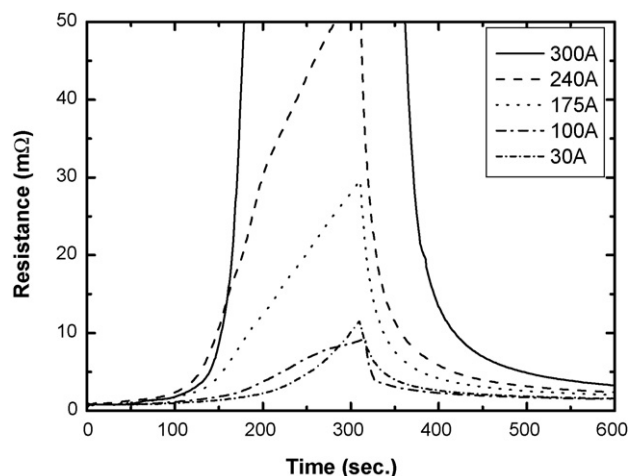


Fig. 10. Effect of operation current on electrolyte membrane dehydration.

### 3.6. Effect of cell temperature

In order to examine the effect of stack temperature on the amount of residual water remaining after the purging process, a series of purging tests was carried out at four different temperatures. First, the fuel cell stack was operated with a load of 175 A for 90 min at 65 °C. After the operation, the load was disconnected and all of the stack inlets and outlets were closed. Then, the temperature of the stack was adjusted to 10, 35, 65, and 90 °C in 2 h. Finally, purging was executed with dry nitrogen for 5 min with flow rates of 3.3 and 9.9 L min<sup>-1</sup> for the anode and cathode, respectively. The residual water remaining for each case is presented in Fig. 11. It is observed that water removal was much more effective at high temperatures compared to low temperatures. Considering that the initial residual water amount just before the purging step was about 28.58 g, as mentioned in Section 3.5, water in the stack was barely discharged when the temperature of the stack was 10 or 35 °C. These phenomena may originate from the low saturated vapor pressure of water in the low temperature cases. At 10 and 35 °C, the saturated water vapor pressure was so low that purging gas could not effi-

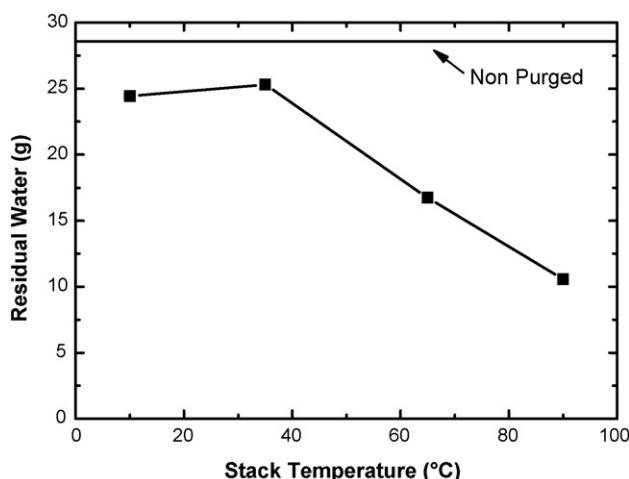


Fig. 11. Effect of stack temperature on the amount of residual water.

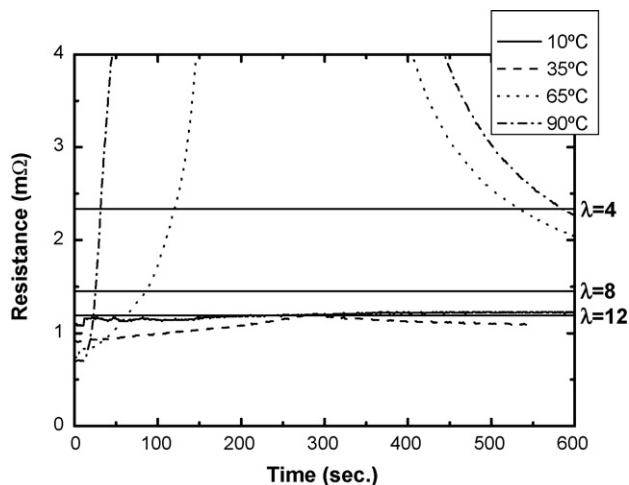


Fig. 12. Effect of stack temperature on electrolyte membrane dehydration.

ciently carry water by vaporization. On the contrary, at 90 °C, the amount of water that was discharged in the form of water vapor was largely due to the high-saturated vapor pressure, resulting in effective water removal, as shown in Fig. 11.

The effect of stack temperature on membrane dehydration is presented in Fig. 12. For temperatures of 10 and 35 °C, there was little change in the water content of the membrane, even though purging was carried out for 5 min. However, the electrolyte membrane was dehydrated rapidly at 90 °C. Therefore, for efficient water removal, it is advantageous to perform the purging step when the stack temperature is high.

#### 4. Summary and conclusions

In order to investigate water removal characteristics by a dry gas purging method, the resistance of the electrolyte membrane and the total amount of residual water in the short stack were measured. The resistance measured by voltage excitation with high frequency was converted to water content in the electrolyte membrane by an empirical correlation. Also, a new method using the phase change of liquid water was developed and successfully adopted to measure the total amount of water in the fuel cell stack. Using these methods, the effects of four factors on water removal were examined: purging time, flow rate of purge gas, operation current, and stack temperature.

Water in the stack was not removed completely even though purging was carried out for long durations up to 20 min. In all cases, residual water hydrated the membrane again right after purging was stopped. When it comes to the effects of purging time, the water removal rate was observed to decrease with increasing purging time. In addition, water removal was more efficient with raising flow rates than with extending purging time when same amount of purge gas was used. The operation cur-

rent also affected the residual water amount. When hydrogen and air were supplied with constant stoichiometry, there was a remarkably larger amount of water remaining in the stack with a low current than with a high current. Therefore, if the fuel cell system in automobiles is operated with light loads such as in the parking mode, water removal methods must be more vigorous. Finally, it is advantageous to perform the purging step when the temperature of the stack is high. Once the stack had cooled to ambient temperatures, water removal by purging was very ineffective.

#### Acknowledgements

This work was supported by the New and Renewable Energy R&D Program and National RD&D Organization for Hydrogen and Fuel Cell under the Korea Ministry of Commerce, Industry, and Energy as a part of the development of 200 kW class PEMFC system for bus (2005-N-F12-P-01). Dr. J.H. Jang, was supported by the Korea Research Foundation Grant funded by the Korean Government (MOEHRD) (KRF-2006-214-D00036) while he was at University of Newcastle upon Tyne.

#### References

- [1] R. Borup, J. Meyers, B. Pivovar, Y.S. Kim, R. Mukundan, N. Garland, D. Myers, M. Wilson, F. Garzon, D. Wood, P. Zelenay, K. More, K. Stroh, T. Zawodzinski, J. Boncella, J.E. McGrath, M. Inaba, K. Miyatake, M. Hori, K. Ota, Z. Ogumi, S. Miyata, A. Nishikata, Z. Siroma, Y. Uchimoto, K. Yasuda, K. Kimijima, N. Iwashita, *Chem. Rev.* 107 (2007) 3904–3951.
- [2] E.A. Cho, J.-J. Ko, H.Y. Ha, S.-A. Hong, K.-Y. Lee, T.-W. Lim, I.-H. Oh, *J. Electrochem. Soc.* 150 (2003) A1667–A1670.
- [3] E.A. Cho, J.-J. Ko, H.Y. Ha, S.-A. Hong, K.-Y. Lee, T.-W. Lim, I.-H. Oh, *J. Electrochem. Soc.* 151 (2004) A661–A665.
- [4] M. Oszcipok, M. Zedda, D. Riemann, D. Geckeler, *J. Power Sources* 154 (2006) 404–411.
- [5] M. Oszcipok, D. Riemann, U. Kronenwett, M. Kreideweis, M. Zedda, *J. Power Sources* 145 (2005) 407–415.
- [6] Q. Yan, H. Toghiani, Y.-W. Lee, K. Liang, H. Causey, *J. Power Sources* 160 (2006) 1242–1250.
- [7] J. Hou, H. Yu, S. Zhang, S. Sun, H. Wang, B. Yi, P. Ming, *J. Power Sources* 162 (2006) 513–520.
- [8] R. Mukundan, Y.S. Kim, F. Garzon, B. Pivovar, 208th ECS Meeting Proceedings, Los Angeles CA, October 16–21, 2005.
- [9] S. He, M.M. Mench, *J. Electrochem. Soc.* 153 (2006) A1724–A1731.
- [10] J. A. Roberts, J. St-Pierre, M. E. van der Geest, A. Atbi, N. J. Fletcher, United States Patent 6,479,177 (2002).
- [11] S. Morishima, E. Tanaka, United States Patent 6,855,444 (2003).
- [12] E. Thompson, R. Fuss, United States Patent 6,887,598 (2002).
- [13] T.E. Springer, T.A. Zawodzinski, S. Gottesfeld, *J. Electrochem. Soc.* 138 (1991) 2334–2342.
- [14] E.A. Cho, U.-S. Jeon, H.Y. Ha, S.-A. Hong, I.-H. Oh, *J. Power Sources* 125 (2004) 178–182.
- [15] H. Wang, M.A. Sweikart, J.A. Turner, *J. Power Sources* 115 (2003) 243–251.
- [16] V. Mishra, F. Yang, R. Pitchumani, *J. Fuel Cell. Sci. Tech.* 1 (2004) 2–9.
- [17] G.J. Van Wylen, R.E. Sonntag, *Fundamentals of Classical Thermodynamics*, 3rd ed., John Wiley & Sons, New York, 1986, pp. 635–651.